JOURNAL OF SOLID STATE CHEMISTRY 11, 190–202 (1974)

High Temperature Study Of Manganese Monoxide

C. PICARD AND P. GERDANIAN

Laboratoire des Composées Non-Stoechiométriques, Université de Paris—Sud, Centre d'Orsay, 91405 Orsay, France

Received November 3, 1973

$g^M_{O_2}$ $(O/Mn)_T$ has been measured accurately by a high temperature thermogravimetric study of physicochemical equilibria between a gaseous oxidoreducing phase and oxide sample. Moreover this method allowed us to know the phase boundaries of manganese monoxide towards Mn_3O_4.

$h^M_{O_2}$ $(O/Mn)_T$ has been directly measured using a high-temperature microcalorimeter. Results obtained remove the uncertainty about values computed by derivation of $g^{M'}_{O_2}$.

From the experimental results, a statistical thermodynamics model has been built up. This model satisfactorily accounts for the high temperature physicochemical properties of manganese monoxide.

Many structural, electric, magnetic, and thermodynamic studies have been carried out on nonstoichiometric compounds and specifically on oxides. Thus, for a number of oxides, the results available are sufficient to build up statistical thermodynamics models which give a satisfactory explanation of their properties.

Of course, these models must take into account all physicochemical results available, but it will only be possible to accept them if the corresponding thermodynamic quantities are in good agreement with experimental data: these data appear as essential in order to test any model and it is of paramount importance to determine them accurately.

The most important thermodynamic functions for oxides are $g^M_{O_2}$, $h^M_{O_2}$, $s^M_{O_2}$, respectively, partial molal Gibbs free energy, enthalpy and entropy of mixing of oxygen in the oxide. As these functions are tied together by the relationship

$$g^M_{O_2} = h^M_{O_2} - Ts^M_{O_2}$$

just two of them need to be known.

$g^M_{O_2} = RT \ln P_{O_2}$ can be directly measured either by the method of physicochemical equilibria between an oxidoreducing gaseous phase and an oxide sample, or by the emf method. These methods are now well known and, when adequately used, the results they yield are generally in agreement.

As for MnO_{1+x} oxides, emf measurements allowed one to determine oxygen partial pressures in equilibrium with the diphasic system MnO–Mn_3O_4 (*1–3*) and the system Mn–MnO (*4*, *5*). Using MnO_{1+x} as measuring electrode, the composition of which is altered coulometrically, Fender and Riley (*3*) determined, on the same sample, log P_{O_2} (T) for various compositions. As was the case with FeO_{1+x} (*6*) the results so obtained suggest to them the existence of several monoxide varieties whose fields would be contiguous. Compositions, however, are given with a fairly important uncertainty: 0.002, that is the fifth part of the extent of the homogeneity range at 1000°C.

Moreover, it seems that the few attempts (*7–10*) towards direct thermogravimetric determination of log P_{O_2} $(O/Mn)_T$ gave only scarce and far too imprecise results.

Generally, all authors give the stoichiometric monoxide as the limit towards manganese of the homogeneity range. Kawahara (*11*, *12*), however, having carried out con-

TABLE I

Field	Ref.		Experimental techniques	$h^M_{O_2}$ kcal mole^{-1}
Mn–$MnO_{1.000}$	Elliott	(*13*)	Emf	−184.5
	Alcock	(*4*)	Emf	−185.9
MnO_{1+x}	Davies	(*9*)	Equilibria	0 (Single values)
	O'Keeffe	(*14*)	Conductimetry	−22 (Single values)
	Bransky	(*10*)	Thermogravimetry	−13.8 (Single values)
	Fender	(*3*)	Emf	3 fields from −130 to −49
$(MnO_{1+x})_l$	Hahn	(*15*)	Equilibria	−118.5 (1248–1540°C)
$-Mn_3O_4$	Blumenthal	(*1*)	Emf	−117.3 (788–1051°C)
	Marion	(*16*)	Equilibria	−112.2
	Fender	(*3*)	Emf	−109.1
	O'Keefe	(*14*)	Conductimetry	−107

ductivity measurements, suggested that there could exist a substoichiometric monoxide corresponding to the *n*-type conduction oxide (III-I) but it has been so far impossible to determine the composition range of existence for this oxide.

On the other hand, $h^M_{O_2}$ determination is more difficult. Indeed, although this function can be computed by derivation of $g^M_{O_2}$, that is

$$\frac{\partial}{\partial(1/T)}\,[g^M_{O_2}/T]_x$$

it is difficult to reckon the accuracy obtained for $h^M_{O_2}$ thus calculated, for the inaccuracy on $g^M_{O_2}$ $(O/M, T)$ is not well known. It is found, moreover, that even when the $g^M_{O_2}$ are in good agreement, the $h^M_{O_2}$ deduced from them are often inconsistent with each other because small differences between the $g^M_{O_2}$ can involve, owing to the derivation, large variations of the $h^M_{O_2}$.

Values for $h^M_{O_2}$ computed by several authors are given in Table I. They differ considerably from each other, especially for the MnO_{1+x} phase.

We believe that direct measurement with a high temperature microcalorimeter is the best procedure to determine $h^M_{O_2}$.

In this work, we strove to determine accurately, the thermodynamic quantities $g^M_{O_2}$ and $h^M_{O_2}$ which, in turn, allowed us to build up a new model in statistical thermodynamics for these oxides.

I. Determination of $g^M_{O_2}$ $(O/Mn)_T$

$g^M_{O_2}$ at 1000, 1050, 1100, and 1150°C for the MnO_{1+x} oxides has been measured using the method of physicochemical equilibria between an oxide sample and a gaseous oxido-reducing phase. Oxide compositions have been determined by means of a thermobalance.

Apparatus, procedure, and results were previously described (*17*). We shall review some of their main characteristics:

(1) We chose Mn_3O_4 as a gravimetric reference. This oxide is stoichiometric at 1000°C in air.

(2) We determined thereafter the composition of the oxides in equilibrium with gaseous mixtures such that $P_{CO_2}/P_{CO} = 0.246$ and we concluded that these oxides are stoichiometric within the accuracy of our experiments, that is $\delta x = 1.5 \times 10^{-4}$.

(3) With these new reference points in hand, we modified the gaseous mixtures in order to cover at each temperature the whole of the monophasic field. Our results are shown in Fig. 1,

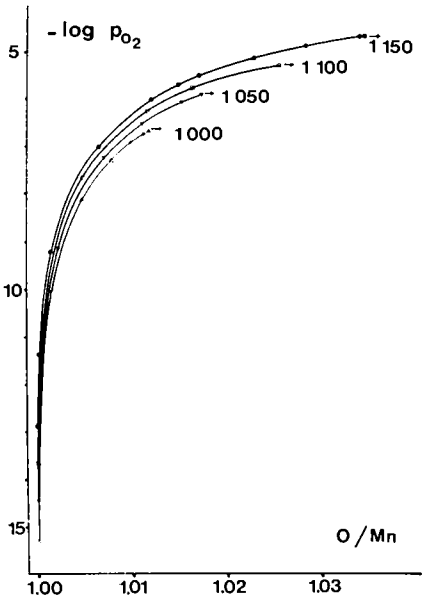

FIG. 1. $-\log_{10} P_{O_2}$ (O/Mn) at 1000, 1050, 1100, 1150°C. Arrows at the end of the isotherms show, for each temperature, the oxygen partial pressure for which we observe an oxidation of MnO_{1+x} in Mn_3O_4.

and are almost identical to those obtained by Bransky (*10*) in the small composition zone $1.000 < O/Mn < 1.004$ he studied. Although our isotherms are in good agreement with those of Hed and Tannhauser (*7*) with $O/Mn < 1.004$, large differences can be found for higher compositions. Moreover, the deviation of our results from those of Fender and Riley (*3*) is never greater than $\delta_x = 0.002$, a satisfactory conclusion if we consider the fact that their compositions are given for $\delta O/Mn = \pm 0.002$.

(4) For each temperature, we bracketed the oxygen partial pressure in equilibrium with the 2 phases MnO–Mn_3O_4 as well as the boundary composition of the monophasic field towards Mn_3O_4.

(5) As oxides vaporize highly for very low P_{O_2}, we could determine neither the limits of the field towards Mn nor the oxygen partial pressures in equilibrium with Mn–MnO. We arrived only at the conclusion that if the equilibrium of oxides with the mixtures H_2–O_2 we used is quickly reached, the width of the substoichiometric field must then be lower than $O/Mn = 0.0002$ at 1000°C.

Lastly, it seems these boundary partial pressures of oxygen can only be determined by the electrochemical procedure.

II. Determination of $h^M_{O_2}$ (O/Mn) 1050°C

We measured partial molal enthalpies of mixing of oxygen in oxides MnO_{1+x} using a Tian–Calvet type microcalorimeter operating at 1050°C. This method has already been used in the laboratory when studying oxides UO_{2+x} (*18*), FeO_{1+x} (*19*), and ZrO_{2-x} (*20*), and it has been demonstrated (*18*) that this procedure is more reliable than the derivation method of $g^M_{O_2}$.

II. 1 Apparatus and Measurements Principle

We blow small quantities of oxygen, δn, of some $4–5 \times 10^{-6}$ mole onto the sample situated in the test tube, in vacuum, inside the microcalorimeter and we measure the small quantities of heat released, δq, ranging from about 0.1 to 1 cal. The microcalorimeter we used has already been described (*18*).

Oxygen quantities, which are constant within 0.8%, are released by means of a hollow handle tap and measured within 0.4% using the calibrated tube of a McLeod gauge.

Samples are rectangular small plates. The sample holder placed into the test tube is made of recrystallized Morgan alumina. It allows us to block all 4 small lateral sides of the sample so that oxygen can be consumed only by both large parallel faces, which in turn gives a better homogenization of oxide during elementary oxidations.

For each release of oxygen, the following reaction can be written:

$$\alpha\ MnO_{1+x} + \delta n\ O_2 \rightarrow \alpha\ MnO_{1+x} + 2\ \delta n/\alpha.$$

It takes place in a container having a constant volume. $\delta \Delta U_{T,V}$ being the internal energy

change for this reaction, it can be shown that:

$$h^M_{O_2} = (\delta \Delta U_{T,V}/\delta n) - RT. \qquad (19)$$

If, on another hand, we can demonstrate that $-\delta \Delta U_{T,V}$ differs very little from the measured heat release, δq, we shall obtain:

$$h^M_{O_2} \simeq -(\delta q/\delta n) - RT.$$

We therefore must measure δq and show that $\delta q \simeq -\delta \Delta U_{T,V}$ in order to determine $h^M_{O_2}$.

II. 2. Preparation of Samples

As we shall point out later (II. 4), it is necessary to prepare dense samples. Moreover they must be rather highly reactive with oxygen. Indeed, it is important that the duration of consumption of oxygen be constant or at least short enough, $t \leqslant 5$ min. If these conditions are not fullfilled, the calibration coefficient varies as well as the endothermic effect (due to residual gases in the test tube) which then can take high values (*21*). Compensations which ought to be brought thereafter are not known with sufficient accuracy.

We tested several methods to make up our MnO samples.

(*a*) *Sintered manganese monoxide samples.* We used $MnO_{1.000}$ in powder prepared from Koch Light Mn_3O_4 as a basis. This powder is pressed then sintered at 1600°C during 5 hr under a pressure of argon of about 200 mm. This sample is then reduced to $MnO_{1.000}$ by heating it at 1050°C during 48 hr in an adequate oxidoreducing atmosphere. Density is then 94% of theoretical density.

Oxygen consumption under the test conditions in the microcalorimeter ranges from 4 to 17 min, according to the composition of the sample. As aforesaid, this is very unfavorable, inasmuch as quantities of heat measured are very low.

Moreover, the δq (O/Mn) curves obtained with these samples do not show any discontinuity when crossing the boundary towards Mn_3O_4, as should be observed, but they exhibit a slow variation on a large composition field. This phenomenon could be attributable to large differences in the consumption rate of oxygen in the oxide. But this does not seem to be the case because of the slow rate of consumption. We rather feel that in these samples, Mn_3O_4 grains temporarily obtained during the release of a small quantity of oxygen cannot easily dissolve in the matrix of MnO: dissolution of these grains would then be the limiting step, not oxygen diffusion in the oxide. It becomes therefore necessary to prepare samples having such a texture that this dissolution will take place quickly.

(*b*) *Reduction of a sintered* Mn_3O_4 *sample.* Pressing and sintering of Koch Light Mn_3O_4 is much easier. Just heating in air at 1400°C to obtain a density reaching 92% of theoretical density told us to continue our efforts.

Unfortunately, reduction of these sintered samples of Mn_3O_4 at 1100°C in an adequate CO–CO_2 mixture gives deeply cracked samples.

(*c*) *Oxidation of manganese.* After numerous attempts, we came to the conclusion that satisfactory samples could be obtained using the following procedure.

We oxidize, at 1150°C, Johnson Matthey electrolytic manganese small plates. Their spectroscopic analysis reveals 40×10^{-6} Mg, 5×10^{-6} Fe, 2×10^{-6} Si and less than 10^{-6} Cu. One face of the plates is smooth, the other is granular. The former has been ground and the plate is oxidized at 1150°C by a gaseous CO–CO_2 mixture having such characteristics that oxide, in equilibrium with the oxygen partial pressure corresponding to this mixture, be in the homogeneity range of the monoxide. After a 2 mo reaction, we cool the furnace and obtain a 0.8 mm thick MnO layer which can easily be separated from its manganese support. After being cut to the sizes of the sample holder, the sample is brought to a composition of $MnO_{1.000}$ in the same conditions as aforesaid.

Oxide samples show big grains on their surface, contrary to samples obtained by sintering.

Consumption rate of oxygen always remains under 5 min, a quite favorable feature if we take into account the preceding remarks. Moreover, the shape of the curves $\delta q/\delta n$ (O/Mn), having a sudden variation when crossing the boundary and constant values in the diphasic field (II. 5) certifies that thermodynamic equilibrium has been really reached. Samples so prepared are therefore convenient for microcalorimeter studies.

II. 3. Measurement of δq: *Rating of the Microcalorimeter*

The calibration coefficient $k = \delta q/S$ of the microcalorimeter must be known before calculating δq from the surface S of a thermogram expressed in arbitrary units. The microcalorimeter can be calibrated using several methods (*18*). We chose the method which seems to be the most reliable and which involves the following relationship:

$$\Delta H = \tfrac{1}{2} \int_{1}^{4/3} h^{M}_{O_2} d(O/Mn)$$

where $h^{M}_{O_2}$ and the integral are dependent only on k and where ΔH is the standard enthalpy of the reaction:

$$6\ MnO + O_2 \rightarrow 2\ Mn_3O_4$$

ΔH can be determined using the data contained in the tables (*17*), i.e., $\Delta H_{1050} = -108.2$ kcal/mole. Any future modification of ΔH_{1050} will obviously result in a change of our calibration coefficient and consequently of our values for $h^{M}_{O_2}$ (O/Mn)

II. 4. Kinetics

As mentioned above, measured quantities of heat δq can be used for the determination of $h^{M}_{O_2}$ only if it can be shown that $\delta q \cong -\delta \Delta U_{T,V}$. This will be the case if, 20 min after the release of a small quantity of oxygen, a duration after which we no longer observe any thermal effect, the oxide has reached a state of homogeneity such that the residual quantity of heat ε to be released or absorbed to reach the perfect state of homogeneity will be negligible (*19*).

This assumption can be checked by considering the oxidation kinetics of our samples by oxidoreducing gaseous mixtures. We performed this study by following, by means of a thermobalance, the variation of weight of the oxide as a function of time. This procedure allows us to obtain $M_t/M_\infty = f(t)$ where M_t and M_∞ are the quantities of oxygen absorbed by the oxide, respectively, after a time t and an infinite duration of reaction. The utilization of results by means of Crank's abacuses (*22*) allows us to compute $\tilde{D}$, chemical diffusion coefficient (Table II).

We shall assume the mean value $\tilde{D}/l^2 = 1.37 \times 10^{-2}$ min^{-1}, i.e., $\tilde{D} = 1.6 \times 10^{-6}$ cm^2 s^{-1}, a result which is in good agreement with those of Bransky (*23*) and Childs (*24*). Obviously enough, this utilization applies only to dense enough samples. Besides, the oxidation kinetics are supposed in the calculus to be limited by the diffusion in the oxide, which results in the determination of a lower boundary for $\tilde{D}$.

In order to deal with the case when small plates are oxidized by oxygen, we use the approximation that all oxygen which is about to diffuse lies on the free surface of the sample. We then use Carslaw's formula (*25*) for an instantaneous plane source to calculate the composition gradient at time t:

$$\frac{C_0 - C}{C_0 - C_\infty} = 1 + 2\sum_{1}^{\infty} (-1)^n \exp\left[-\frac{\tilde{D}\pi^2 n^2 t}{e^2}\right]$$

where C_0 and C_∞ are initial and end compositions and C the composition at time t at a distance e from the surface of the sample, e varying from 0 to a.

After a 20 min reaction in the microcalorimeter this gradient becomes for our 0.8 mm thick small plates

$$\frac{C_0 - C}{C_0 - C_\infty} = 1 - 2\exp\left[\frac{-1.6 \times 10^{-6}\pi^2\, 1200}{(0.04)^2}\right].$$

TABLE II

M_t/M_∞	t (min)	$\tilde{D}t/l^2$	$\tilde{D}/l^2$ $\times 10^2$ min^{-1}
0.6	20.5	0.2809	1.37
0.7	29	0.4070	1.40
0.8	41	0.5700	1.39
0.9	63	0.8464	1.34
0.95	85	1.1449	1.34

It is seen that, in the case of the plate, oxidation is brought by completion by 99.998%. Under these circumstances, due allowance being made for the form of the curve $h^M_{O_2}$ (O/Mn), which will be considered later (II. 5), we deduce that ε is quite negligible compared to δq.

II. 5. Results

We have made 3 series of experiments, 2 of these being carried out in the interval of composition $1.00 \leqslant O/Mn \leqslant 1.03$. When compositions are close to the boundary towards Mn_3O_4, the partial pressure of oxygen is already high enough to allow a reduction of the sample by the dynamic vacuum of a mercury diffusion pump, a fact which in turn would cause a shift of the curve $h^M_{O_2}$ (O/Mn) towards high O/Mn. This phenomenon has indeed been found during preliminary experiments. In order to avoid this reduction, we took care not to create vacuum on samples having a composition $O/Mn > 1.010$.

Our results appear on Fig. 2. Our measurements are reproducible within $\pm$ 1.5 kcal.

We can observe a rapid variation of $h^M_{O_2}$ near the boundary. This variation takes place, in one case, in a composition interval $\Delta x = 0.005$ and, in the other, $\Delta x = 0.003$. We believe this lack of discontinuity at the boundary to come from a small difference of oxygen consumption by the small plate. It has indeed been already demonstrated (*20*) that these differences in the rate of consumption, even though very small, can result in a flattening of the curve $h^M_{O_2}$ which will be all the more marked as the discontinuity is greater. We have therefore rectified our experimental data near the boundary and these rectifications are included in the mean h curve.

Figure 2 shows the values we obtained by derivation of $g^M_{O_2}$ for compositions between $O/Mn = 1.005$ and $O/Mn = 1.010$. Our experimental data being far too imprecise in the area close to stoichiometry, we did not plot them.

We plotted the results arrived at by other authors using a derivation procedure. Our experimental data are diametrically opposed to the values calculated by Fender and Riley (*3*).

Finally, we can note that, in the diphasic field, our results are constant within 1% and are in good agreement with those of the other authors: that is the result of the fact that $g^M_{O_2}$'s are generally well known in the diphasic fields and provide reliable values for $h^M_{O_2}$.

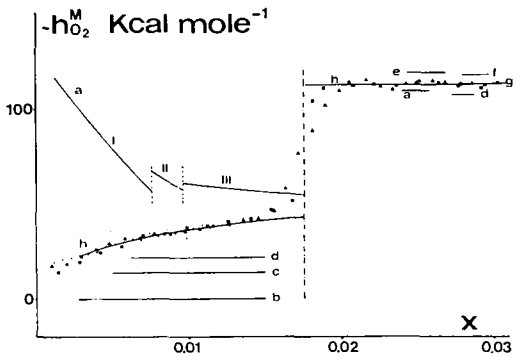

FIG. 2. $-h^M_{O_2}$ kcal/mole (O/Mn) at 1050°C. *Direct measurements:* ● ▲ ■ our experimental data for 3 series of experiments chosen assumed mean curve; *Results obtained by derivation of* $g^M_{O_2}$: □ our results; **a** Fender (*3*), data drawn from $g^M_{O_2}(T)$ O/Mn obtained by the electrochemical method; **b** Davies (*9*); **c** Bransky (*10*); **d** Single values method—O'Keeffe (*14*); and in the diphasic field: **e**—Hahn (*15*); **f**—Blumenthal (*1*); **g**—Marion (*16*).

III. Interpretation of Experimental Results by Means of a Statistical Thermodynamics Model

We interpreted our experimental values for $g^M_{O_2}$ and $h^M_{O_2}$ for oxides MnO_{1+x} by a statistical thermodynamics model. The deviations from stoichiometry of these oxides being rather small, statistical thermodynamics studies are made much easier because the interactions between the various defects can be neglected in this case. It is then well-founded to consider that these latter are randomly dispersed, a fact which allows us to calculate the configurational entropy in the usual way using approximations which are very good in our case.

III. 1. Nature of the Defects

Numerous studies on the variation of electrical conductivity of manganese mon-

oxide as a function of partial pressure of oxygen (*7*, *8*, *11*, *14*, *26*, *27*) at constant temperature reveal that *n*-type conduction changes to *p*-type conduction when partial pressure of oxygen such as P_{CO_2}/P_{CO} is about 1.

Authors distinguish 3 parts in the homogeneity field:

(*a*) An area A corresponding to very low oxygen partial pressures in which the oxide has *n*-type conduction. The fact that the slope of the curve $\log \sigma / (\log P_{O_2})_T$ is $-1/6$ (*8*, *25*, *27*) suggests the presence of doubly ionized manganese interstitials, which according to Kroger's notation is represented by $Mn_i^{\cdot\cdot}$.

Only one author (*11*) finds a slope $-1/8$, a result which can be interpreted as showing the presence of triply ionized manganese interstitials: $Mn_i^{\cdot\cdot\cdot}$.

From his studies on diffusion of manganese in the monoxide, Price (*28*) deduces the existence, in this field, of interstitial manganese $Mn_i^{M\cdot}$, with $m = 1$ or 2.

We should, however, notice that the self diffusion coefficient of Mn does not increase when the partial pressure of oxygen decreases (*11*, *26*) as should happen if $Mn_i^{\cdot}$ was the main defect in the whole of the area A. We can therefore conclude that in the long run, $Mn_i^{\cdot}$ concentration will be greater than the concentration of the other defects (which will be considered later) only in the field of very low P_{O_2} of area A.

Let us now mention that Kawahara (*11*) thinks that this area corresponds to a substoichiometric field, a hypothesis which we previously discussed (*17*).

(*b*) An area B, approx. corresponding to a field of oxygen partial pressures in which $1 < P_{CO_2}/P_{CO} < 1000$, where the oxide exhibits *p*-type conduction; the slope of the curve $\log \sigma/(\log P_{O_2})_T$ is $+1/6$ (*7*, *8*, *11*, *25*, *26*). It is generally considered true that the main defect is then represented by doubly ionized metal vacancies: V''_{Mn}. Price (*28*), too, admits this hypothesis.

(*c*) An area C, with high partial pressures of oxygen, in which conduction is still *p*-type. Price (*28*) admits there the presence of singly ionized metal vacancies, V'_{Mn}. This conclusion is ascertained by Bransky's interpretation (*16*) of his own measurements of equilibrium between oxide and gaseous oxido-reducing phase.

Furthermore, Kofstad (*29*), having studied the experimental results of Hed and Tannhauser (*7*), suggests that there may be non-ionized metal vacancies V^x_{Mn}, in addition to V'_{Mn} vacancies which appear in the area C.

The presence of defects V''_{Mn}, V'_{Mn} and V^x_{Mn} is confirmed after consideration of the slopes $[\partial \log P_{O_2}/\partial x]_T$ of our own isotherms. Let us, however, notice that for our study, both of the latter point defects are quite equivalent to the associations $(V''_{Mn}\ Mn_{\dot{M}n})$ and $(V''_{Mn}\ 2\ Mn_{\dot{M}n})$ where $Mn_{\dot{M}n}$ represents an electron hole localized at the manganese on a normal site.

This latter association has been evidenced by Goodenough (*30*) in a study of the electronic structure of MnO_{1+x}: an isolated cation vacancy would trap a pair of Mn^{3+} ions, one on each side of it, so as to optimize the Madelung energy. On the other hand, we have no experimental data available which would allow us to choose between the V'_{Mn} vacancy and the association $(V''_{Mn}\ Mn_{\dot{M}n})$.

All previous physicochemical results having been reviewed, we would consider the 4 following types of defects: $Mn_i^{\cdot}$, V''_{Mn}, $(V''_{Mn}\ Mn_{\dot{M}n})$ or V'_{Mn}, $(V''_{Mn}\ 2\ Mn_{\dot{M}n})$.

We prefer association $(V''_{Mn}\ Mn_{\dot{M}n})$ to V'_{Mn} vacancy, for this choice has no severe consequence and is expressed only by the introduction of a minor constant into the grand partition function for defects.

To ascertain electric neutrality, we shall in addition admit that $Mn_{\dot{M}n}$ and $Mn'_{\dot{M}n}$ can be found, i.e., electrons localized at the Mn atoms on normal site, in proportion of 2 $Mn'_{\dot{M}n}$ to one $Mn_i^{\cdot}$, of 2 $Mn_{\dot{M}n}$ to 1 V''_{Mn} and of 1 $Mn_{\dot{M}n}$ to one association $(V''_{Mn}\ Mn_{\dot{M}n})$.

For the convenience of the reader, we shall

from now on substitute the following notations for the indexes:

Structural elements	Notation
$Mn_i^{\cdot}$	i
V''_{Mn}	V
$V''_{Mn}\ Mn_{\dot{M}n}$	a
$V''_{Mn}\ 2Mn_{\dot{M}n}$	c
$Mn_{\dot{M}n}$	M·
Mn'_{Mn}	M′
Mn^{x}_{Mn}	M
$O_O{}^{x}$	O

III. 2. Utilization of the Model

We shall use the same method as Gerdanians' (*31*) in his study of UO_{2+x} oxides.

(*a*) The standard state chosen is the perfect stoichiometric crystal having N manganese sites and N oxygen sites: Energy is at zero level when Mn and O atoms are infinitely dispersed, motionless, at their lowest level of energy.

The quantities of energy required to create an interstitial $Mn_i^{\cdot\cdot}$, to fill a vacancy V''_{Mn} or to break an association $(V''_{Mn}\ Mn_{\dot{M}n})$ or $(V''_{Mn}2\ Mn_{\dot{M}n})$ are represented by E_i, E_v, E_a and E_c, respectively. These quantities are positive and correspond to the following reactions:

$$O_O{}^{x} + 3\,Mn^{x}_{Mn} \rightarrow O_\infty + Mn_i^{\cdot\cdot} + 2\,Mn'_{Mn} \qquad E_i$$

$$O_O{}^{x} + 2\,Mn_{\dot{M}n} + V''_{Mn} \rightarrow O_\infty + 2\,Mn^{x}_{Mn} \qquad E_V$$

$$O_O{}^{x} + Mn_{\dot{M}n} + (V''_{Mn}\,Mn_{\dot{M}n}) \rightarrow O_\infty + 2\,Mn^{x}_{Mn} \qquad E_a$$

$$O_O{}^{x} + (V''_{Mn}\,2\,Mn_{\dot{M}n}) \rightarrow O_\infty + 2\,Mn^{x}_{Mn} \qquad E_c.$$

The symbol O_∞ represents oxygen atoms infinitely dispersed and all Mn and all O atoms are motionless at their lowest level of energy.

We shall assume that the various energies E_j are independent of temperature and composition. The numbers of defects are N_i, N_v, N_a and N_c, respectively, their concentrations being $\theta_i = N_i/N$, $\theta_v = N_v/N$, $\theta_a = N_a/N$ and $\theta_c = N_c/N$.

(*b*) All thermodynamical properties of a crystal containing defects can be obtained from its semigrand partition function, Ξ_o.

$\Xi_o\,(T, V, \lambda_o, N) = \sum \text{F.P.}\,(N_j)_{T,V,\lambda o,N}$, $\lambda_o{}^{N} + (N_v + N_a + N_c - N_i)$ where $N + (N_v + N_a + N_c - N_i)$ is the number of oxygen atoms of the system and N_j is the interaction of variables N_i, N_v, N_a and N_c. F.P. (N_j) is the partition function of the system for given N_j and N values. We obtain:

$$\text{F.P.} = \Omega Q \left(\frac{q_i\, q_{M'}^2}{q_M^3\, q_o}\right)^{N_i} \left(\frac{q_M^2 \cdot q_o)}{q_M^2}\right)^{N_v} \times \left(\frac{q_M \cdot q_o q_a}{q_M^2}\right)^{N_a} \left(\frac{q_c q_o}{q_M{}^2}\right)^{N_i} \exp\left[-\frac{E}{KT}\right].$$

E is the additional energy of the system with given Nj compared to the stoichiometric perfect crystal. As seen above the interactions between the defects for small deviations from the stoichiometry can be neglected and E is then equivalent to the energy of formation of these defects:

$$E = N_i\,E_i - N_v\,E_v - N_a\,E_a - N_c\,E_c.$$

Omega is the number of separate configurations of the system with given N_j and N values, having the same values for E.

Q is the partition function of the perfect crystal.

q_1 is the product of the vibrational, electronic and nuclear partition functions for the 1 individual. The first function is calculated from the zero level of energy, which corresponds to a motionless 1 in the crystal, and the 2 other ones are calculated from the lowest level of electronic and nuclear energy.

The semigrand partition function can then be written as follows:

$$\Xi_o = Q\,\lambda_o{}^{N} \sum_{N_j} \Omega\,(q_o\,\lambda_o)^{-N_i+N_v+N_a+N_c} \times Q_i{}^{N_i}\,Q_v{}^{N_v}\,Q_a{}^{N_a}\,Q_c{}^{N_c} \exp\left[-\frac{E}{kT}\right]$$

with

$$Q_i = \left(\frac{q_i\, q_{M'}^2}{q_M{}^3}\right) \qquad Q_v = \left(\frac{q_M^2 \cdot}{q_M{}^2}\right)$$

$$Q_a = \left(\frac{q_M \cdot q_a}{q_M{}^2}\right) \qquad Q_c = \left(\frac{q_c}{q_M{}^2}\right).$$

This function can then take the following form:

$$\Xi_o = Q\,\lambda_o{}^N\,\Xi$$

where Ξ can be considered as the grand partition function of the defects. This latter function will only appear later.

In order to compute Ω, we assume that the various types of defects are randomly dispersed on the sites they can reach, a hypothesis which can be made for small variations from stoichiometry, as we have previously outlined it. Taking the perfect crystal as a basis, the N_i $Mn_i^{\cdot\cdot}$ interstitials and 2 N_i Mn'_{Mn} defects are first introduced, then the N_v vacancies with 2 N_v $Mn_{\dot{M}n}$, thereafter the N_a associations (V''_{Mn} $Mn_{\dot{M}n}$) with N_a $Mn_{\dot{M}n}$ and finally the N_c ($V''_{Mn}2$ $Mn_{\dot{M}n}$) associations. Omega can then be transformed as a product of 4 factors, each one corresponding to one type of defect.

$$\Omega = \Omega_i\,\Omega_v\,\Omega_a\,\Omega_c.$$

We deduce:

$$\Omega_i = \frac{N!}{(N-N_i)!\,N_i!}\,\frac{N!}{(N-2N_i)!\,2N_i!}$$

$$\Omega_v\,\Omega_a = \frac{(N-2N_i)!}{(N-2N_i-N_v)!\,N_v!} \times \frac{(N-2N_i-N_v)!}{(N-2N_i-3N_v-N_a)!\,(2N_v+N_a)!} \times \frac{(2\alpha)^{N_a}\left(\dfrac{N-2N_i-3N_v-N_a}{2}\right)!}{\left(\dfrac{N-2N_i-3N_v-3N_a}{2}\right)!\,N_a!}$$

$$\Omega = \frac{(3\beta)^{N_c}\left(\dfrac{N-2N_i-3N_v-3N_a}{3}\right)!}{\left(\dfrac{N-2N_i-3N_v-3N_a-3N_c}{3}\right)!\,N_c!}$$

in which α is the number of ways of placing one $Mn_{\dot{M}n}$ around one vacancy V''_{Mn} and β the number for $2Mn_{\dot{M}n}$ around V''_{Mn}.

We find that the formulation of Ω depends upon the order of introduction of the various types of defects into the crystal. The differences, however, are negligible for small departures from stoichiometry.

It is known that equilibrium values for N_i, N_v, N_a and N_c correspond to the greatest term of Ξ. These values can be obtained using the four following conditions:

$$\frac{\partial \ln \Xi}{\partial N_j} = 0 \text{ where } N_j = N_i, N_v, N_a, N_c.$$

Four relationships can thus be determined which can be simplified, due allowance being made for the fact that the θ_j's are much lower than 1. We have:

$$\ln \lambda_o = \left[-\ln q_o + \ln \frac{Q_i}{4} - \frac{E_i}{kT}\right] - 3 \ln \theta_i \quad (1)$$

$$\ln \lambda_o = \left[-\ln q_o - \ln Q_v - \frac{E_v}{kT}\right] + \ln \theta_v + 2 \ln(2\theta_v + \theta_a) \quad (2)$$

$$\ln \lambda = \left[-\ln q_o - \ln \alpha\, Q_a - \frac{E_a}{kT}\right] + \ln \theta_a + \ln (2\theta_v + \theta_a) \quad (3)$$

$$\ln \lambda_o = \left[-\ln q_o - \ln \beta Q_c - \frac{E_c}{kT}\right] + \ln \theta_c. \quad (4)$$

θ_i, θ_v, θ_a and θ_c can be computed with these equations as a function of T and λ_o if the terms, contained in the square brackets, of each of the 4 preceding equations are known. $x\,(T, \lambda_o)$ can then be deduced using the relationship:

$$x = \theta_v + \theta_a + \theta_c - \theta_i.$$

We deduce $\lambda_o\ (T, x)$ and, as a consequence, $g^M_{O_2}\ (T, x)$. $g^M_{O_2}$ is, indeed, tied to λ_o by the expression:

$$g^M_{O_2} = 2\,RT \ln \lambda_o + RT \ln (kTQ) + D_{O_2}$$

where $R \ln (kTQ)$ is the "free energy function" at 0°K and D_{O_2} is the dissociation energy for O_2 at 0°K.

$g^M_{O_2}\ (T, x)$ being known, $h^M_{O_2}$ can be determined using the relationship:

$$h^M_{O_2} = \frac{\partial}{\partial 1/T}\left[\frac{g^M_{O_2}}{T}\right]_x$$

or

$$h^M_{O_2} = -2\,RT^2 \frac{\partial}{\partial T}[\ln \lambda_o]_x + D_{O_2} + R\,\frac{\partial}{\partial\, 1/T} \ln (kTQ).$$

When $T = 1323°K$

$$h^M_{O_2} = 107{,}715 - 2RT^2 \frac{\partial}{\partial T}[\ln \lambda_o]_x$$

a result we obtained by adopting Brix and Herzberg's (*32*) value for $D_{O_2} = 117{,}960$ cal/mole and Still and Sinke's (*33*) values for kTQ. We finally come to the following expression for $h^M_{O_2}$ (Appendix)

$$h^M_{O_2 1050} = 123{,}489 \text{ cal} - 2E_i \frac{A_1}{D} - 2E_v \frac{A_2}{D} - 2E_a \frac{A_3}{D} - 2E_c \frac{A_4}{D}$$

with: $A_1 = 2\theta_i(3\theta_v + \theta_a)$
$A_2 = 6\theta_v^2$
$A_3 = 3\theta_a(4\theta_v + \theta_a)$
$A_4 = 6\theta_c(3\theta_v + \theta_a)$
$D = A_1 + A_2 + A_3 + A_4$.

III. 3. Results and Discussion

In order to use this model, the 8 following factors need to be known: Q_i/q_o, $Q_v q_o$, $\alpha Q_a q_o$, $\beta Q_c q_o$, E_i, E_v, E_a, and E_c.

As physicochemical measurements allowing an independent determination of these values were unavailable, we chose them so that experimental measurements of $g^M_{O_2}$ and $h^M_{O_2}$ at 1050°C be in good agreement with theoretical forecasts.

However, this procedure does not allow us to determine the parameters related to the $M_i^{\cdot\cdot}$ defect, since this latter defect is preponderant only for very small deviations from stoichiometry for which we have no thermodynamic measurements available. Therefore, we determined Q_i/q_o and E_i by setting 2 supplementary conditions:

(*a*) The conduction change occurs for the value of $\log P_{O_2} = -13.2$ at 1050°C, a value found by most authors.

(*b*) $h^M_{O_2}$ has a value smaller than −184.5 kcal/mole at the boundary.

The first condition is usable if the mobility of holes and electrons is known. Actually, the knowledge of the ratio of these mobilities is sufficient. This latter ratio can vary considerably from one author to another. We assumed $\mu_n/\mu_p = 1000$, a value which agrees with de Wit's (*34*) and O'Keeffe's (*14*) results.

The second condition is derived from the following considerations: we know that, when crossing the boundary, $h^M_{O_2}$ undergoes a discontinuity, the direction of which depends upon the slope of that boundary in the T (O/M) diagram. Thus, in case of a negatively sloped boundary, $h^M_{O_2}$ decreases when going from the diphasic to the monophasic field.

We do not know the boundary of the MnO_{1+x} field towards Mn at high temperature. We know, however, that at lower temperatures this boundary corresponds to stoichiometric MnO. Furthermore, the substoichiometry is very likely to broaden when temperature rises, a fact which would cause a negatively sloped boundary and a decrease of $h^M_{O_2}$ when crossing the boundary.

Using the tabulated data (*13*), we compute $h^M_{O_2}$ for the diphasic field Mn–MnO, i.e., −184.5 kcal/mole. In the monophasic field, $-h^M_{O_2}$ is likely to start from a value greater than 184.5 and to decrease rapidly to overtake experimental values.

In figs. 3 and 4, we present the theoretical forecasts for $g^M_{O_2}$ and $h^M_{O_2}$ at 1050°C obtained with the following set of parameters:

$$E_i = 215 \text{ kcal/mole}$$

$$E_v = 57 \text{ kcal/mole}$$

$$E_a = 73 \text{ kcal/mole}$$

$$E_c = 96.5 \text{ kcal/mole}$$

$$\log_{10} \frac{Q_i}{4q_o} = -6.06008 - 3 \log_{10} \frac{T}{1323}$$

$$-\log_{10} Q_v q_o = -2.71875 - 3 \log_{10} \frac{T}{1323}$$

$$-\log_{10} \alpha Q_a q_o = -2.55242 - 3 \log_{10} \frac{T}{1323}$$

$$-\log_{10} \beta Q_c q_o = -0.19273 - 3 \log_{10} \frac{T}{1323}.$$

Although the E_j's are temperature independent, according to the hypothesis we have assumed, the same does not hold true in respect of other parameters. Among them, only q_O

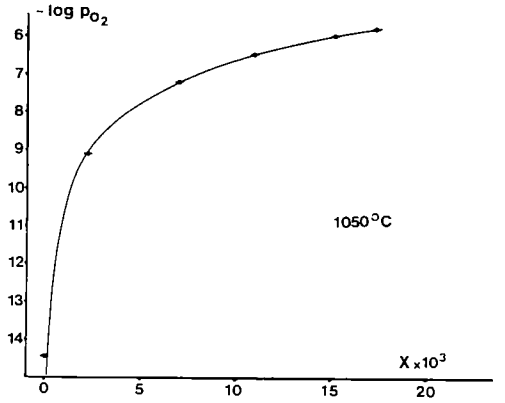

FIG. 3

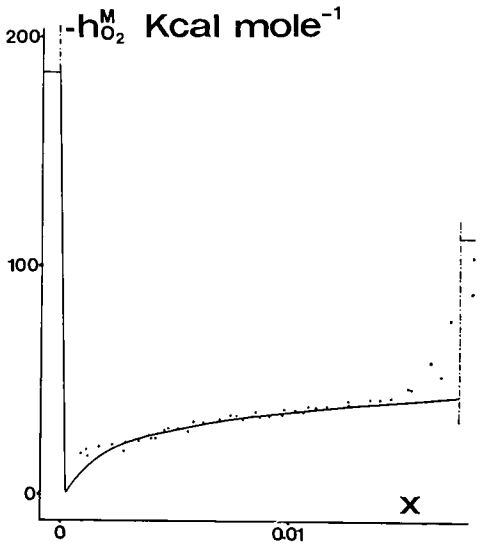

FIG .4

FIGS. 3 and 4. $-\log_{10} P_{O_2}$ $(O/Mn)_{1050°C}$. $-h^M_{O_2}$ $(O/Mn)_{1050}$. We plotted in abscissas x in MnO_{1+x}. For each fig. continuous line represents the function computed at 1050°C according to the model, the points represent our experimental values.

depends upon T. Assuming Einstein's approximation, one deduces:

$$\ln q_o \cong 3 \ln \frac{T}{\theta}$$

whence:

$$[\Delta \ln q_o]^T_{1323} = 3 \ln \frac{T}{1323}.$$

Let us point out that, at 1050°C, one obtains for MnO_{1+x} a boundary composition towards Mn such that $\delta O/Mn = -5.6 \times 10^{-6}$ if one assumes for the oxygen partial pressure in equilibrium with the diphasic mixture Alcock's (*4*) value i.e., $\log P_{O_2} = -26.7$. This result agrees with the conclusions we drew above (*17*).

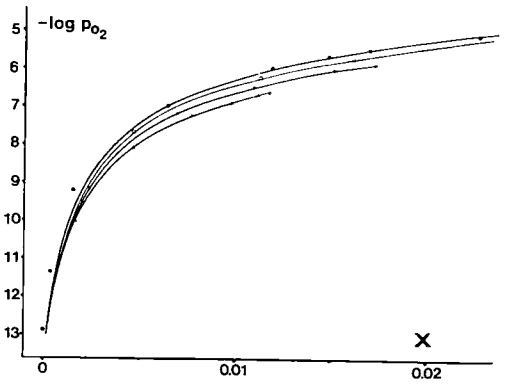

FIG. 5. $-\log P_{O_2}$ (O/Mn) at 1000, 1050, 1100, and 1150°C. We plotted in abscissas x in MnO_{1+x}. Continuous lines have been computed from our model. Points represent our experimental values.

We shall notice that this result depends upon the chosen μ_n/μ_p ratio. However, this value is not decisive. Indeed, if we should have assumed $\mu_n/\mu_p = 100$, a value close to that given by Tannhauser (*36*), our forecasts would have been practically unmodified, with the exception of the width of the substoichiometric range which would become $\delta O/Mn = 12 \times 10^{-5}$. This latter modification is due to the variation of the $Q_i/4q_o$ which would then be such that:

$$\log_{10} \frac{Q_i}{4q_o} = -3.06008 - 3 \log_{10} \frac{T}{1323}.$$

This model satisfactorily accounts for the set of isothermal curves $g^M_{O_2}$ (Fig. 5) with the exception of 2 experimental points at 1150°C for which we observe a weak deviation of the composition of about 5×10^{-4}.

Using this model, we can also compute $\log \sigma$ $(\log P_{O_2})$ at 1050°C, except for a constant.

It has been demonstrated (*8*) that electric conduction in MnO_{1+x} oxides is mainly electronic, hence:

$$\sigma \alpha \left(\frac{\mu_n}{\mu_p}\right) 2\theta_i + (2\theta_v + \theta_a).$$

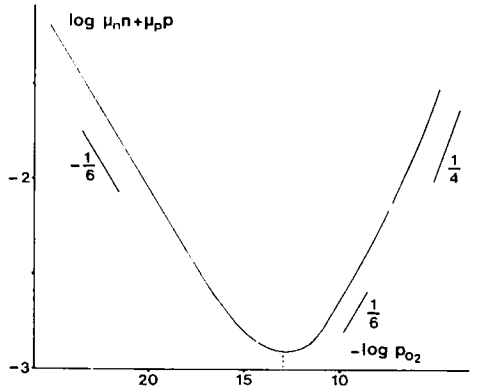

FIG. 6. log σ (log P_{O_2}) at 1050°C, except for a constant, computed from our model (we assumed $\frac{\mu_n}{\mu_p} = 1000$).

We shall assume, as above, $\mu_n/\mu_p = 1000$. The computed curve shown in Fig. 6 accounts for the essential characteristics of the experimental results. Indeed, one can observe a first zone, previously called A, where conduction is n-type with $a - 1/6$ slope; thereafter a B zone with p-type conduction and slope $+ 1/6$; and lastly a C zone with the same type of conduction and $+ 1/4$ slope.

Using the previous energies of formation, we can compute the internal energy change for the following reactions:

$$\tfrac{1}{2}O_2 + 2\,Mn_{Mn}^{x} \rightarrow O_O^{x} + V''_{Mn} + 2\,Mn_{Mn}^{\cdot} \quad E_1$$

$$V'_{Mn} + Mn_{Mn}^{x} \rightarrow V''_{Mn} + Mn_{Mn}^{\cdot}. \quad E_2$$

We find:

$$E_1 = 2\,\text{kcal/mole}$$

$$E_2 = 16\,\text{kcal/mole}.$$

These values are close to those found by Hed and Tannhauser (7), i.e., respectively, -2 and 23 kcal/mole. We can also determine the first ionization energy of a vacancy, i.e., 23.5 kcal/mole.

Appendix

$$h^M_{O_2} = 107{,}715\,\text{cal} - 2\,RT^2\frac{\partial}{\partial T}[\ln \lambda_o]_x.$$

In order to express $\partial/\partial T\,[\ln \lambda_o]_x$ we define:
$a^n = [(\partial \ln \lambda_o)/(\partial T)]\theta_j$ where $\ln \lambda_o$ is given by the expression (n) (III. 2); $n = 1, 2, 3$ or 4.
$b_j^n = [(\partial \ln \lambda_o)/(\partial \theta_j)]_{T,\theta_j'}$ where $\ln \lambda_o$ is given by the expression (n) $j = i, v, a, c$; the θ_j' index indicates that the θ's other than θ_j are constant.

$$C_j = \left[\frac{\partial \theta_j}{\partial T}\right]_x.$$

As $x = \theta_v + \theta_a + \theta_c - \theta_i$, one deduces:

$$\sum [(\partial \theta_j)/(\partial T)]_x = 0. \qquad (5)$$

One then obtains 4 relationships such as:

$$\left[\frac{\partial \ln \lambda_o}{\partial T}\right]_x = \left[\frac{\partial \ln \lambda_o}{\partial T}\right]_{\theta_j} + \sum_{a^n \quad b_j^n \quad c_j} \left[\frac{\partial \ln \lambda_o}{\partial \theta_j}\right]_{T,\theta_j'} \left[\frac{\partial \theta_j}{\partial T}\right]_x. \qquad (6\text{–}9)$$

Using 5–9 relationships one obtains the following system of 4 equations with 4 unknown quantities:

$$a^2 - a^1 = C_i(b_i^1 - b_i^2) + C_v(b_v^1 - b_v^2) + C_a(b_a^1 - b_a^2) + C_c(b_c^1 - b_c^2)$$

$$a^3 - a^2 = C_i(b_i^2 - b_i^3) + C_v(b_v^2 - b_v^3) + C_a(b_a^2 - b_a^3) + C_c(b_c^2 - b_c^3)$$

$$a^4 - a^3 = C_i(b_i^3 - b_i^4) + C_v(b_v^3 - b_v^4) + C_a(b_a^3 - b_a^4) + C_c(b_c^3 - b_c^4)$$

$$0 = -C_i + C_v + C_a + C_c.$$

From relations (1)–(4) (see III. 2) one can compute the a^n's, b_j^n's, C_j's; as $\ln q_o \simeq 3 \ln T/\theta$ one can deduce:

$$\frac{\partial \ln q_o}{\partial T} = \frac{3}{T}$$

there comes:

$$h^M_{O_2\,1050} = 107{,}715 + 6RT - 2E_i\frac{A_1}{D} - 2E_v\frac{A_2}{D} - 2E_a\frac{A_3}{D} - 2E_c\frac{A_4}{D}$$

with $A_1 = 2\theta_i(3\theta_v + \theta_a)$

$A_2 = 6\theta_v^2$

$A_3 = 3\theta_a(4\theta_v + \theta_a)$

$A_4 = 6\theta_c(3\theta_v + \theta_a)$

$D = A_1 + A_2 + A_3 + A_v.$

References

1. R. N. Blumenthal and D. H. Whitmore, *J. Amer. Ceram. Soc.* **44**, 508 (1961).
2. G. C. Charette and S. N. Flengas, *J. Electrochem. Soc.* **115**, 796 (1968).
3. B. E. F. Fender and F. D. Riley, "Chemistry of Extended Defects in Nonmetallic Solids," p. 54, North Holland, Amsterdam (1970).
4. C. B. Alcock and S. Zador, *Electrochem. Acta*, **12**, 573 (1967).
5. K. Schwerdtfeger, *Trans A.I.M.E.* **239**, 1276 (1967).
6. B. E. F. Fender and F. D. Riley, *J. Chem. Solids.* **30**, 793 (1969).
7. A. Z. Hed and D. S. Tannhauser, *J. Electrochem. Soc.* **114**, 314, (1967).
8. N. G. Eror, Thesis Northwestern University Evanston (Illinois) U.S.A. (1965).
9. M. W. Davies and F. D. Richardson, *Trans. Faraday Soc.* **55**, 604, (1959).
10. I. Bransky and N. M. Tallan, *J. Electrochem. Soc.* **118**, 788 (1971).
11. M. Kawahara, thesis, Orsay, November 1967.
12. J. P. Bocquet, M. Kawahara and P. Lacombe. *Compt. Rend. Acad Sci Paris* **265**, 1318 (1967).
13. J. F. Elliott and M. Gleiser, "Thermochemistry for Steelmaking," Addison Wesley, London 1960.
14. M. O'Keefe and M. Valigi, *J. Phys. Chem. Solids* **31**, 947 (1970).
15. W. C. Hahn and A. Muan, *Amer. J. Science* **258**, 66, (1960).
16. Do Quang Khim, Y. Wilbert and F. Marion, *Compt. Rend. Acad. Sci. Paris* **262c**, 756 (1966).
17. B. Touzelin, C. Picard, P. Gerdanian and M. Dode, Séminaires de Chimie de l'état solide, J. Suchet, vol. 6; p. 51 Ed Masson (1972).
18. P. Gerdanian and M. Dode, "Thermodynamics of Nuclear Materials," p. 41, I.A.E.A. Vienne 1967; P. Gerdanian and M. Dode *J. Chim. Phys.* **67**, 1010 (1965); P. Gerdanian, Colloques Internationaux du C.N.R.S. Marseille No. 201 (1971).
19. J. F. Marucco, P. Gerdanian, and M. Dode, *J. Chim. Phys.* **67**, 906 (1970).
20. G. Boureau and P. Gerdanian, *High Temp. High Press.* **2**, 681 (1970).
21. C. Picard, thesis, Orsay, June 1973.
22. Crank, Mathematics of diffusion. Oxford.
23. I. Bransky, N. M. Tallan, J. M. Wimmer and M. Gvishi, *J. Amer. Ceram. Soc.* **54**, 26 (1971).
24. P. E. Childs, L. W. Laub, and J. B. Wagner, *Proc. Brit. Ceram. Soc.* **19**, 29.
25. Carslow and Jeager, "Conduction of Heat in Solids," Oxford.
26. A. Duquesnoy, *Rev. Int. Hautes Temp. Refract.* **3**, 201 (1965).
27. H. Le Brusq., J. J. Oehlig and F. Marion, *Compt. Rend. Acad. Sci. Paris* **266**, 965 (1968).
    H. Le Brusq and J. P. Delmaire, *Rev. Int. Hautes Temp. Refract.* **10**, 15 (1973).
28. J. B. Price and J. B. Wagner Jr. *J. Electrochem. Soc*, **117**, 242 (1970).
29. P. Kofstad, Non stoichiometry, Diffusion and Electrical Conductivity in Binary Metal Oxides, (Burke, Chalmers and Krumhansl, Eds), Wiley-Interscience U.S.A. (1972).
30. J. P. Goodenough, "Progress in Solid State Chemistry," (Reiss, H. Ed.), Vol. 5, Pergamon Press, Oxford (1971).
31. P. Gerdanian, *J. Phys. Chem. Solids* (in press).
32. P. Brix and G. Herzberg, *Canad. J. Phys.* **32**, 110 (1954).
33. D. R. Stull and G. C. Sinke, "Thermodynamic Properties of the Elements," American Chemical Society, Washington D.C. 1956.
34. de Wit. C. Crevecoeur, *Phys. Letter* **25A** 393 (1965).
35. O. Kubaschewski, E. Evans and C. B. Alcock, "Metallurgical Thermochemistry," 4th ed. p. 52, Pergamon Press, Oxford (1967).
36. D. S. Tannhauser, N. M. Tallan and M. Gvishi *Solid State Commun.* **6**, 135 (1968).